MAGNETIC DESIGN STUDIES FOR THE FINAL FOCUS QUADRUPOLES OF THE SUPERB LARGE CROSSING ANGLE COLLISION SCHEME

E. Paoloni, University of Pisa and INFN, Pisa, Italy
S. Bettoni, CERN, Geneva, Switzerland
M. E. Biagini, P. Raimondi, INFN/LNF, Frascati, Italy

Abstract

The final doublets of the Super*B* factory project [1], based on the large crossing angle collision scheme, must provide a pure quadrupolar field on each of the two beams to avoid the high background rates in the detector. Because of the small separation of the low energy (LER) and the high energy (HER) beams the influence of each winding on the other one is not negligible and, for the same space limitation, a multi-layer configuration is not suitable to compensate the high order multipoles. A novel helical-type design has been studied to compensate the fringe field of the quadrupole of one line onto the other one. The 2D algorithm and the 3D finite elements models of this design are presented.

INTRODUCTION

Most of the present, KEK B [2] and DAΦNE [3], and future, Super*B*, colliders exploit the crossing angle scheme to quickly separate the two beams and reach high collision frequency. The magnetic element closest to the Interaction Point (IP) in these machines is usually a horizontal defocusing quadrupole (QD0) common to the two beams. The off-axis particles see a dipolar component which is critical in Super*B* more than in the other machines because of the high strength of the QD0, so that most of the off energy particles produced by bremsstrahlung at the IP hit the beam pipe, producing high multiplicity electromagnetic showers whose cascade enters into the detector. To mitigate their effect massive tungsten shielding should be provided to keep the detector occupancies and radiation damages at a reasonable level [4].

A definitive solution to this problem is to replace the common QD0 with a special quadrupole whose magnetic center lies on the beam reference trajectory for each beam line. In the Super*B* the horizontal separation of the beam lines at the QD0 entrance ($2\,\mathrm{cm} \sim 180\ \sigma_x$) is enough to accommodate only four millimeters of superconducting windings and two cold beam pipe walls, still leaving a reasonable aperture as showned in Fig. 1. Themechanical constraints are too tight for a conventional septum magnet and to compensate the cross-talk among the quadrupoles of the two lines, therefore a novel design has been studied.

CROSS TALK COMPENSATION

Let consider a current density $\mathbf{j}$ concentrated in a unit radius cylinder with axis z. Let $\mathbf{j} = \hat{z} j_z(\varphi)\delta(r-1)$ be

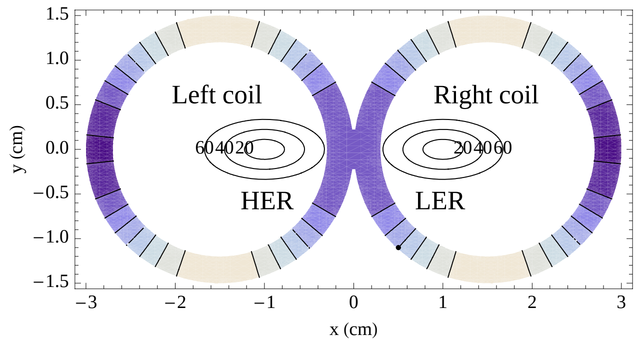

Figure 1: Schematic $x - y$ cross section of the double quadrupole. $20, 40, 60\ \sigma_x$ beam envelopes at the QD0 entrance are sketched. Gray-tones represents the intensity of j_z.

invariant under z translation and let φ be the angle in polar coordinates with respect to the cylinder axis. The magnetic field B is independent from the z coordinate and can be expressed at point $\zeta \equiv x + iy$ as:

$$B(\zeta) \equiv B_y(\zeta) + iB_x(\zeta) = k \int_0^{2\pi} d\varphi\, \frac{j_z(\varphi)}{\zeta - e^{i\varphi}}$$

where x and y are the transverse coordinates. Using the algebraic relation:

$$\frac{1}{\zeta - e^{i\varphi}} = \frac{1}{\zeta} - \frac{1}{\zeta^2}\frac{1}{\frac{1}{\zeta} - e^{-i\varphi}}$$

it can be derived that:

$$B(\zeta) = -\frac{1}{\zeta^2}\overline{B}(\frac{1}{\overline{\zeta}}) + \frac{k}{\zeta}\int_0^{2\pi} d\varphi\, j_z(\varphi) \qquad (1)$$

where $\overline{\zeta}$ is the ζ complex conjugate. If ζ is outside the cylinder then $1/\overline{\zeta}$ in inside and vice-versa, therefore eq. 1 relates the far and near field generated by $\mathbf{j}$, so that the set of functional equations can be written:

$$\begin{cases} B_\mathrm{L}(\zeta) + B_\mathrm{R}(\zeta - \Delta) &= B_\mathrm{L}(\zeta) - \frac{1}{(\zeta-\Delta)^2}\overline{B_\mathrm{R}}(\frac{1}{\overline{\zeta}-\Delta}) \\ &= B_\mathrm{L}^\mathrm{tot}(\zeta) \\ B_\mathrm{R}(\zeta) + B_\mathrm{L}(\zeta + \Delta) &= B_\mathrm{R}(\zeta) - \frac{1}{(\zeta+\Delta)^2}\overline{B_\mathrm{L}}(\frac{1}{\overline{\zeta}+\Delta}) \\ &= B_\mathrm{R}^\mathrm{tot}(\zeta) \end{cases}$$

where Δ is the distance among the cylinder centers, B_L (B_R) represents the field generated by the left (right) coil and $B_{\mathrm{L}}^{\mathrm{tot}}$ ($B_{\mathrm{R}}^{\mathrm{tot}}$) is the total, assigned, field present inside the left (right) coil. The succession of functions:

$$\begin{aligned} B_{\mathrm{L}n}(\zeta) &= \frac{1}{(\zeta-\Delta)^2}\overline{B_{\mathrm{R}n}}\left(\frac{1}{\overline{\zeta}-\Delta}\right) + B_{\mathrm{L}}^{\mathrm{tot}}(\zeta) \\ B_{\mathrm{R}n}(\zeta) &= \frac{1}{(\zeta+\Delta)^2}\overline{B_{\mathrm{L}n-1}}\left(\frac{1}{\overline{\zeta}+\Delta}\right) + B_{\mathrm{L}}^{\mathrm{tot}}(\zeta) \\ B_{\mathrm{L}0}(\zeta) &= 0 \end{aligned}$$

converges quite fast to the solution of eq.(1). For typical values of Δ and target fields $n = 20$ gives solutions with 10^{-8} accuracy. The left field sources j_{L_z} is then determined according to the Ampère law:

$$\begin{aligned} j_{\mathrm{L}_z}(\varphi) &= \lim_{\delta\to 0}\left[B_{\mathrm{L}}(e^{i\varphi}(1+\delta)) - B_{\mathrm{L}}(e^{i\varphi}(1-\delta))\right]\ e^{i\varphi} \\ &= \left[B_{\mathrm{L}}(e^{i\varphi}) + \frac{1}{e^{2i\varphi}}\overline{B}_{\mathrm{L}}\left(\frac{1}{e^{-i\varphi}}\right)\right]\ e^{i\varphi} \end{aligned}$$

The winding shape to obtain such a current distribution is obtained using the AML-like technique [5], which consists in superimposing to this current density distribution a solenoidal one:

$$\mathbf{j} = \left[\hat{z}\ j_{\mathrm{L}_z}(\varphi) + \hat{z}\frac{\Delta z}{2\pi} + \hat{\varphi}\right]\ \delta(r-1)$$

The winding shape $\mathbf{x}(\lambda)$ is then readily obtained solving the differential equation:

$$\mathbf{x}'(\lambda) = \mathbf{j}(\mathbf{x})$$

To cancel-out the inner solenoidal field and the outer $1/\zeta$ field a second layer is wound reversing the solenoidal superimposed current:

$$\mathbf{j} = \left[\hat{z}\ j_{\mathrm{L}_z}(\varphi) - \hat{z}\frac{\Delta z}{2\pi} - \hat{\varphi}\right]\ \delta(r-1)$$

Finally the right field sources is obtained with the same technique starting from B_{R}.

3D SIMULATIONS

Magnetic models of the windings obtained applying the algorithm described in the previous section have been simulated in 3D [6]. The windings shape has been optimized to improve as much as possible the field quality in 3D in the central part of the magnet and to minimize the end-effect at the extremities of the coils. Assuming a NbTi strand the margin to quench of the best configuration has therefore been determined using as parameters the strand properties and the radius of the windings both at 4.2 K and 1.9 K. These parameterizations will be used to adapt the design to the Super*B* final focus requests.

Field Quality

The windings shape in 3D has been optimized varying the minimum angle of the wire with respect to the z axis

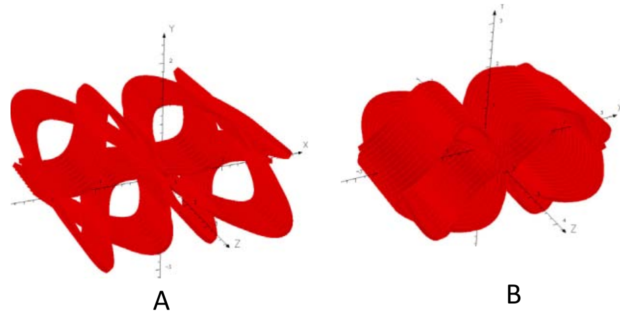

Figure 2: Some of the simulated configurations. A and B correspond to an increasing scan number.

from 84 ° to 45 °. In Fig. 2 some of the simulated configurations are shown. For each model at several $\overline{z}$ the vertical component of the magnetic field around the center of the coils on the mid-plane, (x_C,0,$\overline{z}$) has been computed and fitted according to:

$$B_y(x - x_C, 0, \overline{z}) = \sum_{i=0}^{N} b_i (x - x_C)^i \qquad (2)$$

The higher order terms normalized to the quadrupole B_i/B_1 have therefore been calculated as:

$$\frac{B_i}{B_1} \equiv \frac{b_i (x - x_C)^{i-1}}{b_1}, i = 2, 3, \ldots \qquad (3)$$

The third order polynomial allowed to obtain norm of residuals normalized to the quadrupolar field of the order of 10^{-6}. The second and the third order coefficients of the most promising configurations are shown in Fig. 3. The

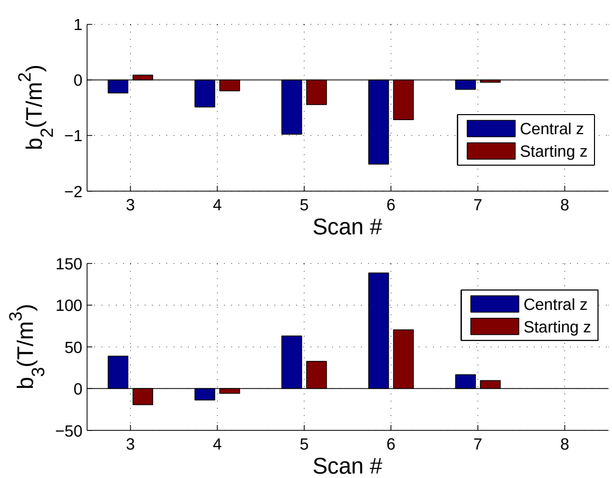

Figure 3: b_2 and b_3 of the best configurations of the scan at half of the length of the coil (Central z) and at the extremities of the windings (Starting z).

configurations 4 and 7 allow for having a field quality better than 10 parts over a million. For J equal to 500 A/mm ^{2} they have a similar gradient (b_1 = 31.46 T/m for 4 and 31.44

T/m for 7), maximum field in the conductor (0.50 T for 4 and 0.52 T for 7) and field quality in the central part of the windings, but configuration 7 has been preferred because of the better end-effect and the higher radius of curvature, both advantageous for the mechanics and the degradation. In Table 1 the second and third term of the field expansion of this configuration are shown. This configuration

Table 1: Higher order terms normalized to the quadrupole of the best configuration of the scan.

	z center	z start
B_2/B_1	$-2.72 \cdot 10^{-5}$	$-1.36 \cdot 10^{-5}$
B_3/B_1	$+1.33 \cdot 10^{-5}$	$+1.52 \cdot 10^{-5}$

has therefore been used to study the margin to quench of coils built according to this kind of design.

Margin to Quench

At a fixed geometry (1 cm internal radius, 2 mm conductor thickness) and NbTi strand properties (1 mm x 1 mm wire, Cu/SC equal to 0) the gradient and the maximum field in the conductor have been determined as a function of J. Imposing a target gradient, the necessary current density is determined from the first function and, known J, the maximum field in the conductor is calculated from the second one. This pair (J,$|B|_{MAX}$) defines the working point of the coils, which is compared to the NbTi [7] critical curve at a fixed temperature as a function of Cu/SC both at 4.2 K and 1.9 K. The dependence of the margin to quench on Cu/SC is shown in Fig. 4. Assuming a Cu/SC between 1.0 and 1.5

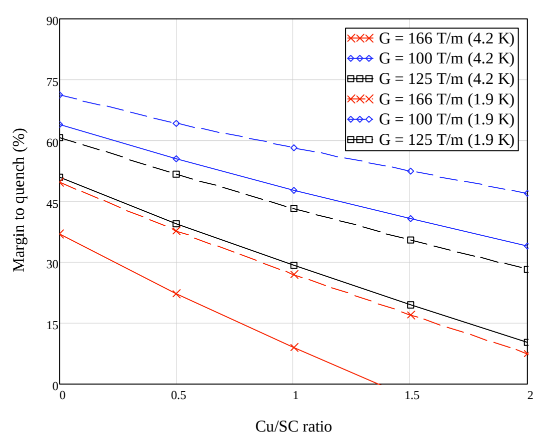

Figure 4: Margin to quench as a function of Cu/SC for several gradients (internal radius of the coils equal to 1 cm) at 4.2 K and 1.9 K.

a gradient of 125 T/m at 4.2 K and of 166 T/m at 1.9 K are feasible with a margin between 20% and 30%.

The dependence of the margin to quench on the coils geometry (variable internal radius) at a fixed Cu/SC has been also studied. The result is shown in Fig. 5. In the Super*B* final focus this layout would allow to produce gradient equal to 100 T/m at 4.2 K and 125 T/m at 1.9 K.

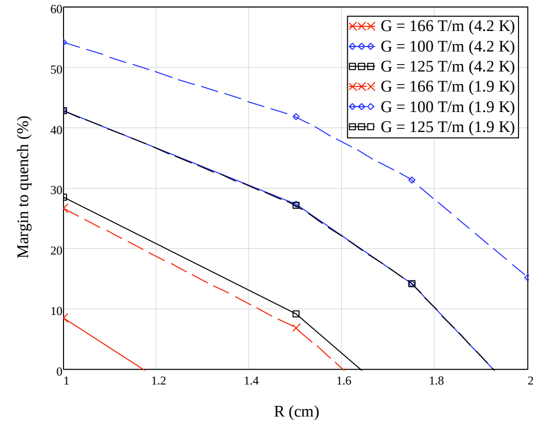

Figure 5: Margin to quench as a function of the internal radius of the coils (Cu/SC assumed equal to 1) at 4.2 K and 1.9 K.

CONCLUSIONS

A new configuration based on one quadrupole for each beam line of the Super*B* final focus has been recently proposed to eliminate the high background due to off energy particles. Due to the very tigh requests of this design (no more than 3 mm for the conductors for each quadrupole and distance between the axes of the magnets of only 1 cm), the cross talk between the quadrupoles is not negligible and, for the same reason, a multi-layer design is not feasible. In this paper an algorithm to compensate this effect has been presented. 3D simulations showed that with this technique an excellent field quality (better than 10 part per million) can be achieved. Also the margin to quench has been studied using as parameters the aperture radius and the copper over superconductor ratio both at 4.2 K and at 1.9 K. This will allow to adapt the design to the Super*B* final focus design requests. The authors wish to thank Luca Argenti for the many insightful conversations and advices.

REFERENCES

[1] J. Seeman *et al.*, "Design of a 1036cm-2s-1 Super*B* factory" WEPP039 this conference.

[2] Y. Funakoshi, "Performance of KEKB with crab cavities" WEXG01 this conference.

[3] C. Milardi *et al.*, "DAFNE Setup and Operation with the Crab Waist Collision Scheme" WEPP036 this conference.

[4] M. Bona *et al.*, "Super*B*: A High-Luminosity Asymmetric e^+e^- Super Flavor Factory. Conceptual Design Report," arXiv:0709.0451 [hep-ex].

[5] Advanced Magnet Lab, AML, internet site `http://magnetlab.com/technology`.

[6] Opera Vector Fields analysis (Tosca), software for electromagnetic design, version 11.0, Vector Fields Ltd., Oxford, England, Vector Fields Inc., Illinois, USA.

[7] L. Bottura, "A practical fit for the critical surface of NbTi," IEEE Transactions on Applied Superconductivity, Vol. 10, no. 1, March 2000.